FULL TITLE
ASP Conference Series, Vol. **VOLUME**, **YEAR OF PUBLICATION**
NAMES OF EDITORS

Optical light curves of RS Oph (2006) and hydrogen burning turnoff

Izumi Hachisu[1], Mariko Kato[2], Seiichiro Kiyota[3], Katsuaki Kubotera[3], Hiroyuki Maehara[3], Kazuhiro Nakajima[3], Yuko Ishii[4], Mari Kamada[4], Sahori Mizoguchi[4], Shinji Nishiyama[4], Naoko Sumitomo[4], Ken'ichi Tanaka[4], Masayuki Yamanaka[4], Kozo Sadakane[4]

[1] *Dept. of Earth Sci. & Astr., Univ. of Tokyo, Tokyo 153-8902, Japan*
[2] *Keio Univ.* [3] *Var. Star Obs. League in Japan* [4] *Osaka Kyoiku Univ.*

Abstract. We report a coordinated multi-band photometry of the RS Oph 2006 outburst and highlight the emission line free y-band photometry that shows a mid-plateau phase at $y \sim 10.2$ mag from day 40 to day 75 after the discovery followed by a sharp drop of the final decline. Such mid-plateau phases are observed in other two recurrent novae, U Sco and CI Aql, and are interpreted as a bright disk irradiated by the white dwarf. We have calculated theoretical light curves based on the optically thick wind theory and have reproduced the early decline, mid-plateau phase, and final decline. The final decline is identified with the end of steady hydrogen shell-burning, which turned out at about day 80. This turnoff date is consistent with the end of a supersoft X-ray phase observed with *Swift*. Our model suggests a white dwarf mass of $1.35 \pm 0.01\ M_\odot$, which indicates that RS Oph is a progenitor of Type Ia supernovae. We strongly recommend the y-filter observation of novae to detect both the presence of a disk and the hydrogen burning turnoff. Observational data of y magnitudes are provided here together with other multi-wavelength light curve data.

1. Optical observation of RS Oph (2006)

It is well known that the X-ray turnoff time is a good indicator of the white dwarf (WD) mass (e.g., Hachisu & Kato 2006a,b). When the hydrogen shell-burning atop the WD extinguishes, a supersoft X-ray phase ends (e.g., Krautter et al. 1996). In a visual light curve, however, this turnoff is not clear because many strong emission lines contribute to it. To avoid such contamination to the continuum flux, we have observed RS Oph with the Strömgren y-band filter. The y-filter is an intermediate bandpass filter designed to cut the strong emission lines in the wide V bandpass filter, so that its light curve represents the continuum flux of novae (e.g., Hachisu & Kato 2006b). We have further modeled the light curve of RS Oph and have estimated the WD mass by fitting our modeled light curve with the observation.

Optical observations were started just after the discovery of the 2006 outburst (Narumi et al. 2006). Each observation are listed in Tables 1 and 2. We have put a special emphasis on the Strömgren y filter to avoid contamination by the strong emission lines. These y filters were made by Custom Scientific,

Inc.,[1] and distributed to each observer by one of the authors (M. Kato). Kiyota, Kubotera, Maehara, and Nakajima (VSOLJ members) started observation on 2006 February 13 and obtained data for y magnitudes from 2006 February 17 until 2007 June 20. The Osaka Kyoiku University (OKU) team obtained V and y magnitudes of 42 nights starting from 2006 February 17 until 2006 November 17. The magnitudes of this object were measured by using the local standard star, TYC2 5094.92.1 (Kiyota) or TYC2 5094.283.1 (the other observers). We adapted the brightness and color of ($y = V = 9.57$, $B - V = 0.56$) for TYC2 5094.92.1 and ($y = V = 9.35$, $B - V = 1.23$) for TYC2 5094.283.1 from the Tycho2 catalog.

Table 1. Optical Data of Osaka Kyoiku Univ.

Days	JD	y	err.	obs.	V	err.	obs.
6.33	3784.33	6.98	0.02	11	6.47	0.01	6
16.30	3794.30	8.26	0.01	14	7.61	0.01	5
24.25	3802.25	8.83	0.01	11	8.02	0.02	10
31.30	3809.30	9.48	0.01	10	8.76	0.01	10
34.27	3812.27	9.65	0.01	10	8.90	0.02	10
37.24	3815.24	9.69	0.02	10	8.94	0.03	10
41.25	3819.25	9.92	0.01	10	9.22	0.03	10
48.22	3826.22	10.08	0.01	10	9.39	0.02	10
51.21	3829.21	10.07	0.01	11	9.45	0.01	10
55.22	3833.22	10.11	0.01	10	9.54	0.01	10
72.19	3850.19	10.20	0.01	10	9.80	0.02	10
73.19	3851.19	10.28	0.02	10	9.82	0.01	10
78.14	3856.14	10.36	0.02	10	9.98	0.02	10
80.13	3858.13	10.54	0.01	10	10.08	0.01	10
83.13	3861.13	10.68	0.03	10	10.23	0.02	10
98.09	3876.09	11.47	0.03	10	11.00	0.01	10
99.13	3877.13	11.47	0.01	10	11.03	0.01	10
102.03	3880.03	11.52	0.02	11	11.10	0.03	10
108.08	3886.08	11.88	0.07	10	11.40	0.02	10
112.17	3890.17	11.93	0.04	10	11.45	0.02	10
115.17	3893.17	11.85	0.04	10	11.38	0.02	10
122.15	3900.15	11.80	0.03	10	11.41	0.02	10
128.16	3906.16	11.99	0.06	5	11.56	0.11	4
152.04	3930.04	12.01	0.06	10	11.71	0.03	9
153.15	3931.15	11.97	0.03	10	11.69	0.04	10
177.01	3955.01	11.68	0.02	10	11.47	0.03	10
184.04	3962.04	11.83	0.02	10	11.62	0.02	10
192.96	3970.96	11.67	0.02	10	11.48	0.02	10
220.93	3998.93	11.53	0.02	10	11.38	0.01	10
227.97	4005.97	11.70	0.04	10	11.51	0.02	10
238.95	4016.95	11.68	0.03	10	11.49	0.03	10
247.90	4025.90	11.69	0.03	10	11.60	0.03	10
248.90	4026.90	11.76	0.04	10	11.61	0.02	10
257.93	4035.93	12.00	0.04	48	–	–	–
261.90	4039.90	11.90	0.03	10	11.70	0.05	10
264.88	4042.88	11.67	0.02	10	–	–	–
266.94	4044.94	11.54	0.07	7	–	–	–
267.91	4045.91	11.61	0.16	6	–	–	–
268.90	4046.90	11.50	0.03	10	–	–	–
269.88	4047.88	11.33	0.03	10	–	–	–
270.88	4048.88	11.30	0.02	10	–	–	–
278.86	4056.86	11.42	0.05	10	–	–	–

2. WD mass, Mid-plateau phase, and distance

Our main results are summarized as follows (see Hachisu et al. 2006, for more details);

1. The y-band light curve observed can be divided into three phases: (a) the early, fast-decline phase until day 40 after the discovery (we assume here $t_{\rm OB} =$

[1]See http://www.customscientific.com.

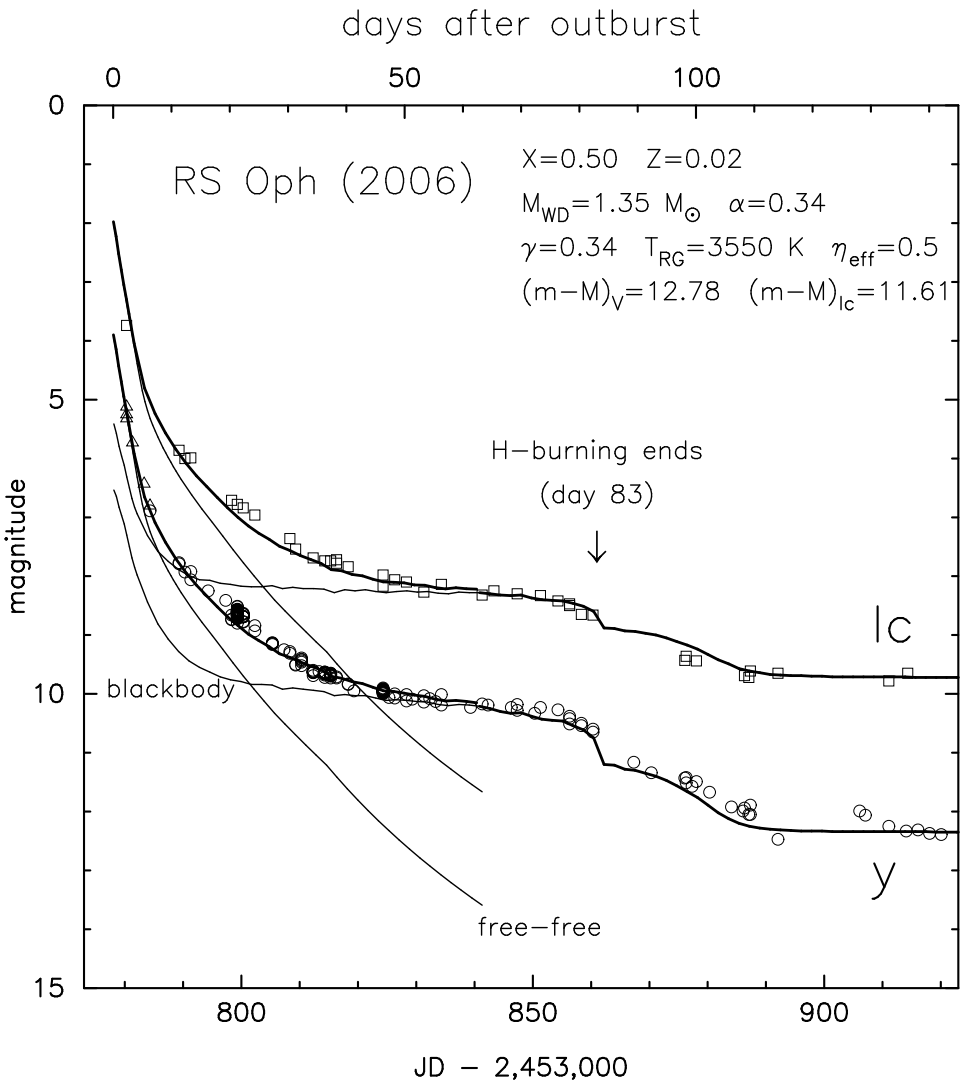

Figure 1. y (*open circles*)and Ic (*open squares*) light curves for the RS Oph (2006). Thick solid lines are combined free-free and blackbody.

JD 2,453,778.0 as the origin of time as the outburst), (b) a mid-plateau phase at $y \sim 10.2$ mag from day 40 to day 75, and (c) the final decline starting on day 75. This mid-plateau phase is first identified by our y light curve. The y and Ic light curves are shown in Figure 1.

2. Assuming that the binary consists of a red giant companion, a WD, and a disk around the WD, we calculate theoretical light curves and reproduce the observed y and I_c light curves. Also we assume that free-free emission from the WD envelope (optically thin plasma) dominates in the early decline phase while the irradiated disk (photospheric) component dominates in the mid-plateau phase. The fitting results are shown in Figure1 (see also Figures 2 and 3 of Hachisu et al. 2006).

Table 2. Optical Data of VSOLJ

Days	JD	B	V	y	vis.	R	I_c
1.36	779.36	-	-	-	4.46	-	-
2.33	780.33	-	5.23	-	5.11	4.46	3.74
3.36	781.36	-	5.73	-	5.61	-	-
4.33	782.33	-	-	-	5.70	-	-
5.36	783.36	-	6.43	-	6.32	-	-
6.35	784.35	7.53	6.80	6.89	6.70	6.06	-
7.33	785.33	-	-	-	6.93	-	-
9.33	787.33	-	-	-	7.10	-	-
10.35	788.35	-	-	-	7.10	-	-
11.32	789.32	8.18	7.46	7.78	7.16	6.04	5.86
12.34	790.34	8.33	7.68	7.93	-	-	6.00
13.31	791.31	8.54	7.66	7.99	7.43	6.05	5.99
15.33	793.33	-	-	-	8.00	-	-
16.33	794.33	8.85	8.00	8.25	-	6.11	-
19.29	797.29	8.99	8.29	8.41	-	6.24	-
20.30	798.30	9.08	8.37	8.71	8.10	6.55	6.71
21.30	799.30	8.97	8.38	8.63	8.10	6.61	6.78
22.29	800.29	9.22	8.39	8.69	-	6.97	6.84
23.26	801.26	-	-	-	8.30	-	-
24.27	802.27	9.21	8.53	8.88	-	6.75	6.96
27.30	805.30	-	8.82	9.14	-	-	-
29.31	807.31	9.68	9.03	9.25	-	6.91	-
30.28	808.28	9.70	8.97	9.29	8.10	7.15	7.36
31.26	809.26	9.91	9.18	9.51	-	7.31	7.54
32.29	810.29	9.89	9.08	9.44	-	7.72	-
34.25	812.25	10.14	9.22	9.63	-	7.48	7.69
35.32	813.32	10.14	9.46	9.62	-	7.33	-
36.24	814.24	10.13	9.26	9.65	9.60	7.58	7.74
37.26	815.26	10.11	9.29	9.68	-	7.53	7.74
38.25	816.25	10.10	9.41	9.72	9.50	7.78	7.75
40.27	818.27	10.30	9.56	9.84	-	7.72	7.84
41.28	819.28	10.44	9.80	9.95	9.40	7.64	-
42.27	820.27	-	-	-	9.50	-	-
46.26	824.26	10.44	9.60	9.95	-	8.00	8.07
47.25	825.25	10.60	9.93	10.06	9.90	7.84	-
48.28	826.28	10.53	9.86	10.03	-	7.99	8.06
50.26	828.26	10.56	9.88	10.06	9.90	8.05	8.10
51.24	829.24	10.64	9.93	10.09	10.10	7.93	-
53.23	831.23	10.61	9.84	10.08	-	8.20	8.27
54.22	832.22	10.70	9.95	10.08	-	8.02	-
55.22	833.22	10.71	9.98	10.13	-	8.04	-
56.27	834.27	10.69	9.95	10.10	-	8.21	8.14
61.21	839.21	10.87	10.06	10.23	-	8.23	-
63.18	841.18	10.72	9.89	10.17	-	8.58	8.32
64.22	842.22	10.86	10.07	10.19	10.20	8.23	-
65.26	843.26	10.77	10.00	-	-	8.49	8.25
68.22	846.22	10.99	10.16	10.23	-	8.38	-
69.25	847.25	10.92	10.10	10.23	-	8.46	8.30
72.18	850.18	11.07	10.21	10.33	-	8.44	-
73.26	851.26	10.93	10.08	10.23	-	8.63	8.33
76.27	854.27	11.04	10.17	10.27	-	8.67	8.42
78.24	856.24	11.13	10.26	10.44	-	8.78	8.48
80.17	858.17	10.97	10.33	10.52	-	8.85	8.65
82.25	860.25	11.36	10.49	10.62	10.80	8.89	8.66
89.16	867.16	11.81	11.01	11.16	-	9.29	-
92.16	870.16	11.99	11.13	11.34	-	9.51	-
98.15	876.15	12.15	11.20	11.45	-	9.88	9.39
99.19	877.19	12.30	11.34	11.57	11.20	9.83	-

3. The decline rate of the free-free light curve and the hydrogen burning turnoff date depend not only on the WD mass but also on the chemical composition of the envelope (Hachisu & Kato 2006b). First we have fitted the decline with $M_{\rm WD} = 1.35\ M_\odot$ assuming a chemical composition of $X = 0.5$, and then examined two other cases of hydrogen content, $X = 0.70$ and $X = 0.35$, and found that the best fit models are obtained for $M_{\rm WD} = 1.36$ and $1.34\ M_\odot$, respectively. So we conclude that the WD mass is $1.35 \pm 0.01\ M_\odot$.

4. The turnoff date of steady hydrogen shell-burning is day ~ 80, which is consistent with the end of a supersoft X-ray phase observed with *Swift* (Hachisu et al. 2007). The sharp drop of the final decline phase strongly indicates the epoch when the hydrogen shell-burning ends.

Table 2. Optical Data of VSOLJ (continued)

Days	JD	B	V	y	vis.	R	I_c
100.08	878.08	12.24	11.14	11.49	-	10.02	9.44
102.13	880.13	12.40	11.43	11.67	11.10	9.93	-
106.12	884.12	12.64	11.69	11.92	-	10.22	-
108.18	886.18	12.69	11.65	11.96	-	10.33	9.69
109.17	887.17	12.68	11.65	11.99	-	10.35	9.66
110.09	888.09	-	-	-	11.80	-	-
111.14	889.14	-	-	-	11.40	-	-
114.09	892.09	12.79	11.48	12.47	-	10.45	9.65
115.12	893.12	-	-	-	11.70	-	-
127.18	905.18	-	-	-	11.90	-	-
128.07	906.07	12.83	11.79	11.99	-	10.41	-
129.06	907.06	12.99	11.86	12.06	-	10.49	-
133.05	911.05	13.09	11.76	12.25	-	10.67	9.78
136.13	914.13	13.05	12.12	12.33	-	10.71	9.65
137.99	915.99	13.22	12.18	12.31	-	10.78	-
140.04	918.04	13.22	12.17	12.37	-	10.77	-
141.99	919.99	13.22	12.21	12.39	-	10.77	-
152.09	930.09	13.12	11.86	12.07	12.20	10.60	9.60
153.18	931.18	13.17	11.76	11.97	-	10.48	9.58
155.00	933.00	13.13	-	12.07	-	10.57	-
164.00	942.00	13.24	12.14	12.31	-	10.83	-
165.00	943.00	13.28	12.01	12.19	-	10.85	9.71
166.00	944.00	13.24	12.08	12.26	-	10.82	-
167.07	945.07	13.18	11.91	12.02	-	10.71	9.64
168.02	946.02	13.18	12.01	12.19	11.90	10.74	-
172.00	950.00	13.05	11.79	11.92	-	10.57	-
173.05	951.05	13.02	11.70	11.80	-	10.49	9.44
174.00	952.00	12.97	11.69	11.90	-	10.54	9.47
175.04	953.04	12.91	11.59	11.69	-	10.44	9.39
176.10	954.10	12.98	11.53	11.59	-	10.41	9.37
178.99	956.99	12.95	11.66	11.76	-	10.49	-
180.03	958.03	12.94	11.56	11.74	-	10.52	9.46
182.15	960.15	-	11.55	-	-	10.49	9.44
182.99	960.99	13.00	11.77	11.85	-	10.58	-
184.00	962.00	12.97	11.71	11.81	-	10.62	9.50
188.11	966.11	13.00	11.71	11.86	-	10.60	9.51
190.00	968.00	13.04	11.79	11.87	-	10.59	-
192.98	970.98	12.86	11.64	11.76	-	10.49	-
193.99	971.99	12.82	11.56	11.70	-	10.43	-
199.95	977.95	12.88	11.68	11.79	-	10.53	-
201.03	979.03	-	11.43	-	-	10.43	9.55
202.02	980.02	12.92	11.85	11.88	-	10.62	9.51
203.06	981.06	12.95	11.77	11.92	11.90	10.64	9.51
204.96	982.96	13.08	11.97	12.02	-	10.75	-
205.94	983.94	13.18	12.02	12.13	-	10.81	-
210.95	988.95	13.39	12.20	12.28	-	10.89	9.74
216.00	994.00	-	11.51	-	-	-	9.41
218.96	996.96	12.97	11.49	11.55	-	10.35	9.36
219.95	997.95	12.93	11.49	11.60	-	10.36	-
220.93	998.93	12.97	11.47	11.61	-	10.35	-
223.92	1001.92	12.91	11.44	11.46	-	10.33	9.31
224.92	1002.92	12.97	11.52	11.64	-	10.42	-
227.93	1005.93	12.95	11.46	11.61	11.70	10.46	9.40
230.94	1008.94	-	-	-	11.80	-	-
236.90	1014.90	13.03	11.66	11.81	-	10.51	-
237.94	1015.94	12.96	11.54	11.62	11.80	10.44	9.40
238.89	1016.89	-	-	-	11.90	-	-
239.91	1017.91	12.89	11.50	11.53	-	10.43	9.36
244.93	1022.93	12.91	11.56	11.55	-	10.44	9.37
245.91	1023.91	12.92	11.59	11.61	-	10.48	9.41

5. From the light curve fitting, we obtain a white dwarf mass of $1.35 \pm 0.01\ M_\odot$, which is close to the Chandrasekhar mass ($1.38\ M_\odot$, see, e.g., Nomoto 1982). This suggests that RS Oph is a progenitor system of Type Ia supernovae.
6. The distance is estimated to be 1.3-1.7 kpc from the y and I_c light curve fittings in the late phase of the outburst.
7. Finally, we strongly recommend the y-filter observation of novae to detect both the presence of a disk and the hydrogen burning turn-off.

References

Hachisu, I., & Kato, M. 2001, ApJ, 558, 323

Table 2. Optical Data of VSOLJ (continued)

Days	JD	B	V	y	vis.	R	I_c
251.90	1029.90	-	-	-	11.90	-	-
254.88	1032.88	-	-	-	11.90	-	-
255.88	1033.88	-	-	-	11.80	-	-
259.90	1037.90	-	-	-	11.90	-	-
265.88	1043.88	12.84	11.62	11.60	-	10.59	-
268.90	1046.90	12.70	11.45	11.42	-	10.42	9.44
269.87	1047.87	12.77	11.35	11.42	-	10.31	-
270.87	1048.87	12.70	11.29	11.36	-	10.24	-
271.85	1049.85	12.72	11.31	11.37	-	10.27	-
273.89	1051.89	12.66	11.26	11.26	-	10.21	9.25
274.87	1052.87	12.78	11.29	11.35	-	10.26	-
276.87	1054.87	12.88	11.38	11.51	-	10.36	-
330.36	1108.36	-	11.42	11.50	-	10.49	9.37
336.34	1114.34	-	11.36	11.45	-	10.49	9.40
337.32	1115.32	-	11.11	-	-	10.35	9.29
341.33	1119.33	-	11.21	11.29	-	10.34	9.30
345.33	1123.33	-	11.44	-	-	10.52	9.47
347.32	1125.32	-	11.61	11.70	-	10.65	9.52
355.35	1133.35	13.15	11.96	12.08	-	11.01	9.85
357.32	1135.32	-	12.02	12.11	-	11.15	9.96
358.32	1136.32	-	11.79	11.81	-	11.01	9.81
360.33	1138.33	12.62	11.80	11.91	-	10.96	9.83
361.32	1139.32	-	11.81	11.81	12.00	11.03	9.89
365.32	1143.32	-	11.36	11.42	-	10.64	9.57
366.35	1144.35	-	-	-	12.00	-	-
368.35	1146.35	12.74	11.54	11.56	12.00	10.58	-
369.31	1147.31	-	11.32	11.38	-	10.54	9.43
370.32	1148.32	12.14	11.40	11.32	-	10.57	9.45
372.35	1150.35	12.60	11.34	11.38	-	10.33	-
374.35	1152.35	12.74	11.44	11.45	-	10.43	-
375.29	1153.29	-	11.30	11.34	-	10.44	9.36
377.36	1155.36	-	-	-	11.70	-	-
378.32	1156.32	12.30	11.15	11.17	-	10.30	9.24
380.30	1158.30	-	11.12	11.24	-	10.26	9.23
381.30	1159.30	12.53	11.26	-	-	10.27	-
382.31	1160.31	12.67	11.46	11.49	11.80	10.53	9.38
383.32	1161.32	12.37	11.26	11.26	-	10.29	9.21
388.27	1166.27	12.74	11.51	11.58	-	10.55	-
389.28	1167.28	12.69	11.52	11.56	-	10.58	-
390.26	1168.26	12.71	11.50	11.55	-	10.55	-
391.27	1169.27	12.94	11.68	11.59	-	10.71	-
394.20	1172.20	12.65	11.75	11.54	-	10.56	-
400.28	1178.28	12.63	11.45	11.47	-	10.43	-
409.29	1187.29	-	-	-	11.60	-	-
416.22	1194.22	12.63	11.45	11.49	-	10.47	-
418.23	1196.23	12.66	11.35	11.37	-	10.37	-
422.20	1200.20	12.45	11.24	11.20	-	10.23	-
424.21	1202.21	12.53	11.25	11.26	-	10.27	-
432.30	1210.30	12.56	11.20	11.17	-	10.12	9.10
442.25	1220.25	12.26	10.95	11.05	-	10.02	-
450.14	1228.14	12.33	11.16	11.15	-	10.22	-
454.28	1232.28	12.33	11.14	11.17	-	10.23	-
460.24	1238.24	12.34	11.22	11.13	11.30	10.23	-
462.25	1240.25	-	10.95	-	-	-	-
463.26	1241.26	12.19	10.98	10.95	-	10.06	-
474.08	1252.08	12.23	10.99	10.99	-	10.09	-
479.12	1257.12	-	-	-	11.20	-	-
480.12	1258.12	12.49	11.15	11.21	-	10.21	-
483.15	1261.15	-	-	-	10.60	-	-
485.19	1263.19	12.11	10.91	-	-	-	-
489.24	1267.24	-	11.32	-	-	-	-
494.17	1272.17	12.57	11.40	-	-	10.43	-

Hachisu, I., & Kato, M. 2006a, ApJ, 642, L53
Hachisu, I., & Kato, M. 2006b, ApJS, 167, 59
Hachisu, I. et al. 2006, ApJ, 651, L141
Hachisu, I., Kato, M., & Luna, G. J. M. 2007, ApJ, 659, L153
Krautter, J., Ögelman, H., Starrfield, S., Wichmann, R., & Pfeffermann, E. 1996, ApJ, .456, 788
Narumi, H., Hirosawa, K., Kanai, K., Renz, W., Pereira, A., Nakano, S., Nakamura, Y., & Pojmanski, G. 2006, IAU Circ., 8671
Nomoto, K. 1982, ApJ, 253, 798